

# MONTHLY WEATHER REVIEW

JAMES E. CASKEY, JR., Editor

Volume 88  
Number 5

MAY 1960

Closed July 15, 1960  
Issued August 15, 1960

## WIND SPEED AND AIR FLOW PATTERNS IN THE DALLAS TORNADO OF APRIL 2, 1957

WALTER H. HOECKER, JR.

U.S. Weather Bureau, Washington, D.C.

[Manuscript received March 15, 1960; revised June 10, 1960]

### ABSTRACT

A composite distribution of tangential and upward components of air flow is determined by tracing particles of debris and cloud tag movements in scaled movies of a tornado. The greatest tangential speed measured is 170 m.p.h. and the greatest upward speed derived is 150 m.p.h. A distribution of the convergent radial component of motion in the lower 600 ft. of the vortex is synthesized and used to generate a vertical speed distribution which nearly duplicates the observed vertical speed distribution.

The observed radial distribution of the vertical component of relative vorticity at three levels is shown and convergence at the 500-ft. radius is computed using the synthesized radial speed distribution. Three-dimensional trajectories of air parcels in the lower portion of the vortex are also shown.

### 1. INTRODUCTION

For many decades the speed of the wind in the tornado has been an object of great curiosity, and many indirect means have been used to estimate at least the maximum wind speed near the ground in a given tornado and many theoretical studies have estimated the speed distribution in the tornado vortex. In this investigation the scaling of high-quality tornado movies (some scenes taken with a 100 times magnifying telephoto lens) has allowed the determination of derived wind speeds in the Dallas, Tex., tornado of April 2, 1957, by tracing the time rate of movement of cloud fragments and debris elements circulating around this tornado.

A limited distribution of the speeds of the tangential and vertical wind components over a range of radii and heights above the ground in the space occupied by the Dallas tornado has been derived. Of necessity, the measurements were not simultaneous, being made in several periods where the earliest and latest measurements were separated by about 19 minutes. Therefore, the speed distributions shown in this paper are composites

of speeds from different times and it will be shown that speeds obtained late in the tornado lifetime do not fit the pattern of those obtained predominantly in the early part. The fact that the condensation envelope, or visible tornado, was suspended a few hundreds of feet aloft during most of this measuring period made possible some measurements in a region that ordinarily is obscured. Wind speeds quoted for the tornado are relative to the tornado, and are those of the tracer elements except where corrections have been applied to some vertical speeds. Wind speed assumptions relative to tracer speeds are explained in the text. Radial symmetry is assumed for all speed distributions described in this paper.

### 2. TANGENTIAL WIND SPEEDS

The tangential components of wind around the Dallas tornado are discussed in this section. It is to be kept in mind that the data points are located where by chance tracer particles were located and that the highest speed measured was not necessarily the highest speed existing in the tornado. It is also well to remember that this



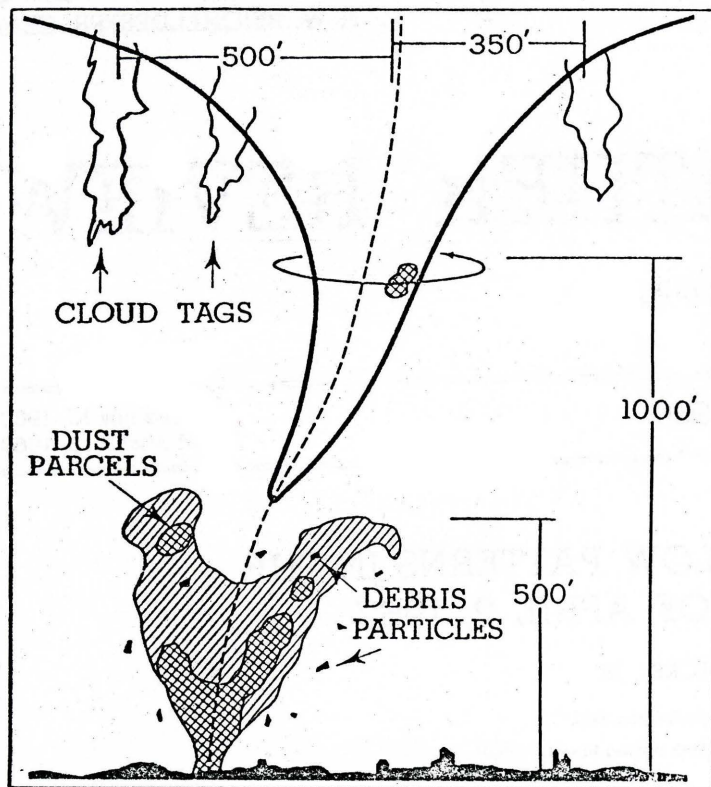


FIGURE 1.—The various types of elements used as air flow tracers in the wind speed measurements of the Dallas tornado of April 2, 1957.

tornado was relatively small, but at the same time was fairly stable in character; at the ground its damage path was at times spotty (c.f. [5]).

Figure 1 shows the various types of elements that were used as air flow tracers in measuring the speed. In the upper portion were the cloud tags and fragments rotating around the tornado; and in the lower portion, that is, in and around the debris cloud, were the dust parcels and pieces of debris. In some instances the speed of roughness elements on the surface of the funnel was measured and in one instance the speed of rotation of a flattened funnel tip was determined; both gave speeds on the funnel surface. It was assumed that the cloud elements and dust or mud-spray parcels were moving at the actual speed of the air in which they were imbedded. For the more or less solid debris particles, it was presumed that the wind speed was at least as fast as that of the particle of debris used as a tracer. The radii of the paths of the cloud tags were found by measuring the extreme left- or right-hand projected distance that the tags extended from the tornado center as they rotated around it. The radii of the paths of solid debris particles not determinable as described above, were obtained by observing their horizontal projected speed distributions relative to the center of the tornado. Trial and error fitting of observed projected speed distribution curves to a range of computed projected speed curves allowed an estimation of the

radius. The tornado appeared to be in approximately the same stage of development for most of the observations.

The distribution of tangential speeds, determined as described above, is shown in figure 2 on a graph of height versus radius. Isotachs are smoothed to these data points. The average position of the condensation envelope relative to most of the data points is shown as a dot-dash line across the upper left-hand part of the graph. The center of the tornado is, of course, along the vertical scale at zero radius. The greatest derived tangential speed was 170 m.p.h., and was found at a radius of 130 ft. and an elevation of 225 ft. This does not mean that the speed was limited to 170 m.p.h., since other tracers not considered here might have indicated greater speeds. The greatest derived low-level speed was 122 m.p.h., which was found at an elevation of 70 ft. and a radius of 90 ft. Other than the fact that the tangential speed at the earth's surface is required to be zero, the distribution of speed between the ground and the level of the 122 m.p.h. datum point is not known. Unfortunately, these data are bunched in space and some interpolation has been necessary, particularly between 500 and 1000 ft. in elevation and inward from the 400-ft. radius.

For the information of the reader the data points of figure 2 are coded as to the type of element traced in obtaining the distribution of tangential speeds. The triangles indicate that solid debris particles were tracked. These were mainly some uniformly sized rectangularly shaped thin sheets of material about 4 x 8 ft. in size and were located below 500 ft. in elevation and inward from the 300-ft. radius. The dots indicate cloud tags and dust parcels and the squares show where the surface of the condensation funnel itself was used. The two stars indicate non-uniformly sized solid debris tracers.

In considering the distribution of wind speed, one must remember that this analysis is not unique and that there are groups of data, for example some of those in the region around 1000 ft. in elevation and 500 ft. in radius, which do not fit the analysis as presented here. The isotachs could be redrawn to fit some of the other data points more closely than they are fitted in this analysis. However, if one did this it would not greatly change the pattern as shown in figure 2, but only change the radii of some isotachs. The analysis shows a band of maximum speed starting at about 60 ft. in elevation and 70 ft. in radius and increasing in diameter with height such that at the 1200-ft. level the radius is about 260 ft. Possibly the maximum speed band continued downward and inward from the lowest datum point shown in figure 2. Generally, the radial distribution of tangential speed resembles that of the Rankine combined vortex where speed increases with decreasing radius to a certain radius inside of which the speed decreases linearly to zero at the center.

The observed distribution also shows the tendency for an increase in speed with elevation for the region outside of the maximum speed band. Attention is called to the



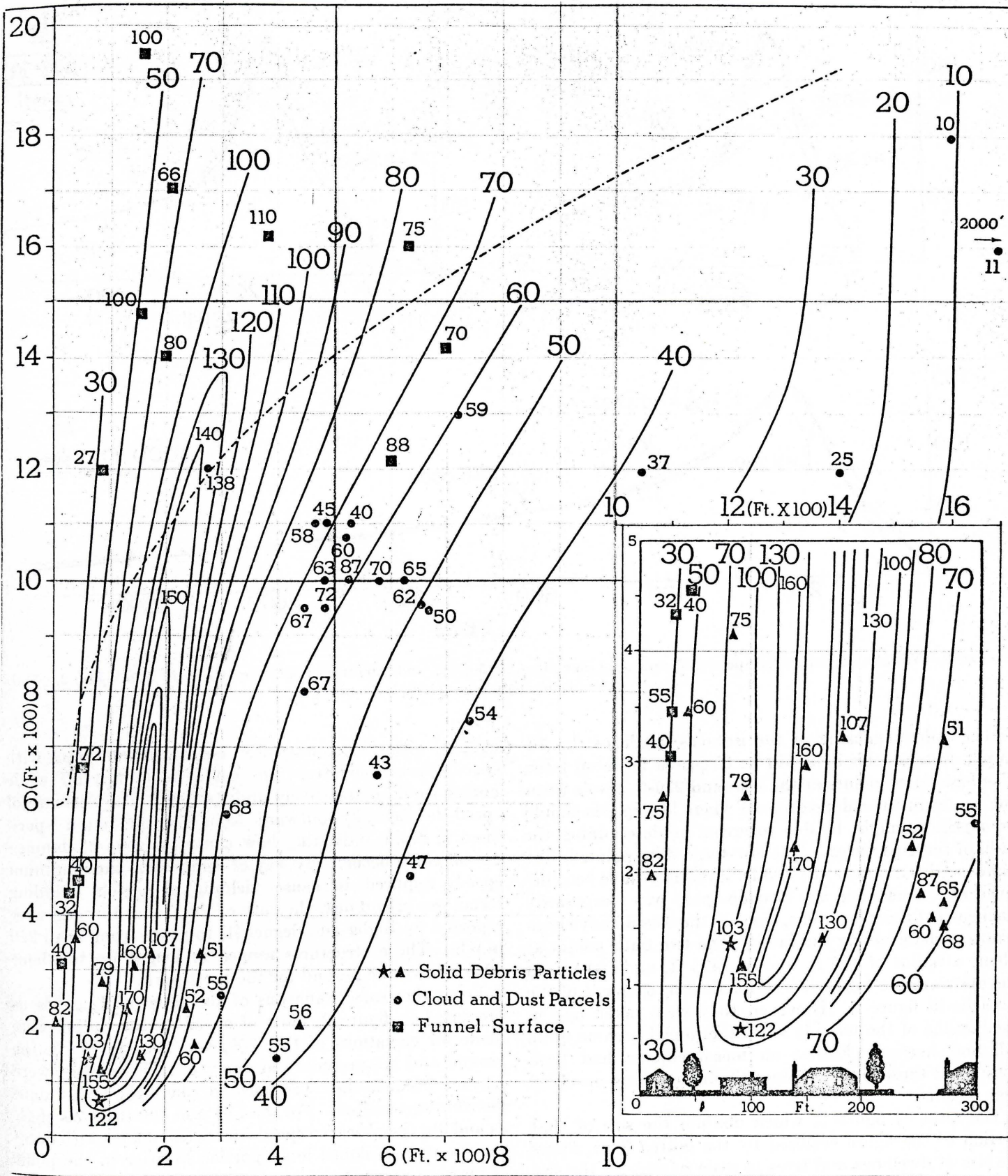


FIGURE 2.—Distribution of derived tangential speed from the center of the tornado to a radius of 2000 ft. and from near the ground to about 1800 ft. in elevation.



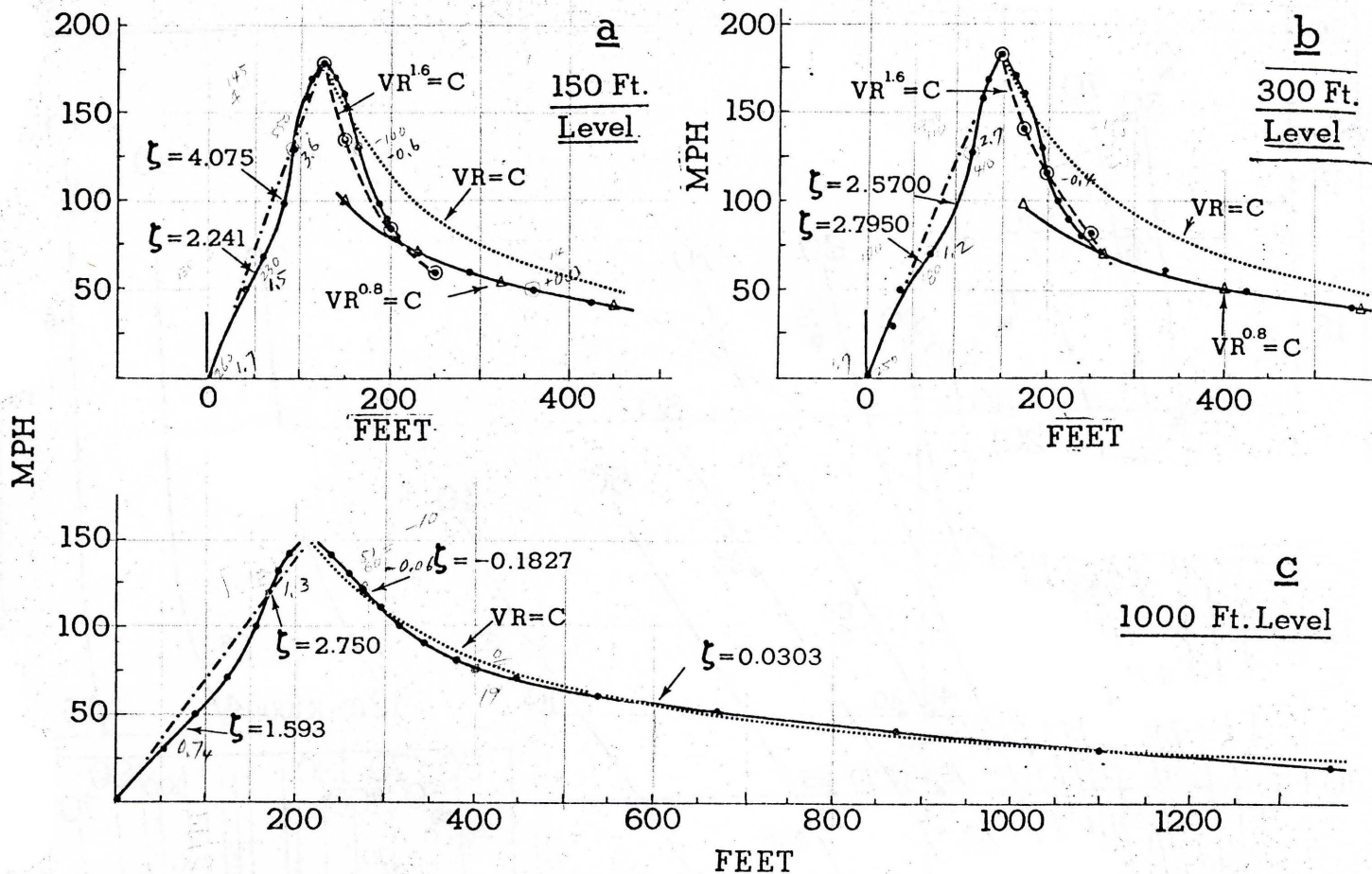


FIGURE 3.—Variation of tangential speed with radius for elevations of 150, 300, and 1000 ft. as taken from the analysis of figure 2. Data taken from analyzed isotachs.

rather sudden packing of the isotachs inside of the 70-m.p.h. isotach; this item will be discussed in detail later. The high-speed points at the 200- and 270-ft. levels (near the center in the enlarged inset) where low speeds should be expected, might be due to errors in determining the radii of these particles. The low-speed data points in the high-speed band near the 300-ft. level may have been derived at a time when the tornado speed was temporarily slackened at those locations, or again there could have been errors in determining the radii. The two data points at about a radius of 150 ft. and at 1475 ft. and 1940 ft. in elevation are too high in speed for the arrangement of the isotachs in figure 2. However, they were taken late in the lifetime of the tornado when the funnel became quite tall and narrow. Earlier no measurements had been possible at those locations since the funnel cloud occupied that region.

The inset of figure 2, which doubles the size of that portion of the figure enclosed by the dotted lines, shows the size of dwellings and trees to scale relative to the size of the isotach speed distribution. One-half of a city block extends from the left edge of the drawing to the 220-ft. mark. The rapid increase of speed upward into the band of maximum speed in the lowest 100 ft. above the ground

coupled with the second-power increase of wind force with speed, shows how tree tops could be broken off while houses would be relatively undisturbed. The decrease of speed horizontally outward from the maximum speed band is rapid, indicating how a narrow zone of damage cut-off could occur. By way of comparison the minimum speeds required to cause yielding of certain building structures in and near the path of the Dallas tornado were reported by Bigler and Segner [1] to range from 55 to 220 m.p.h. These structures ranged in height up to about 20 ft. above the ground for the most part.

From the isotach analysis of the tangential speeds as presented in figure 2, plots of speed versus radius were made for elevations of 150, 300, and 1000 ft. above the ground and are presented in figure 3. These levels were selected because they were located where the better data distributions existed. For the 150- and 300-ft. levels (figs. 3a and 3b) the observed speed curves (solid lines with dots) show a steeply-sloped inner portion exterior to the point of maximum speed out to about the 250-ft. radius and a shallowly-sloped outer portion in the region exterior to about the 250-ft. radius. A definite break in the slopes between the inner and outer portions is evident. A comparison of these curves with the  $VR = \text{Constant}$  curves



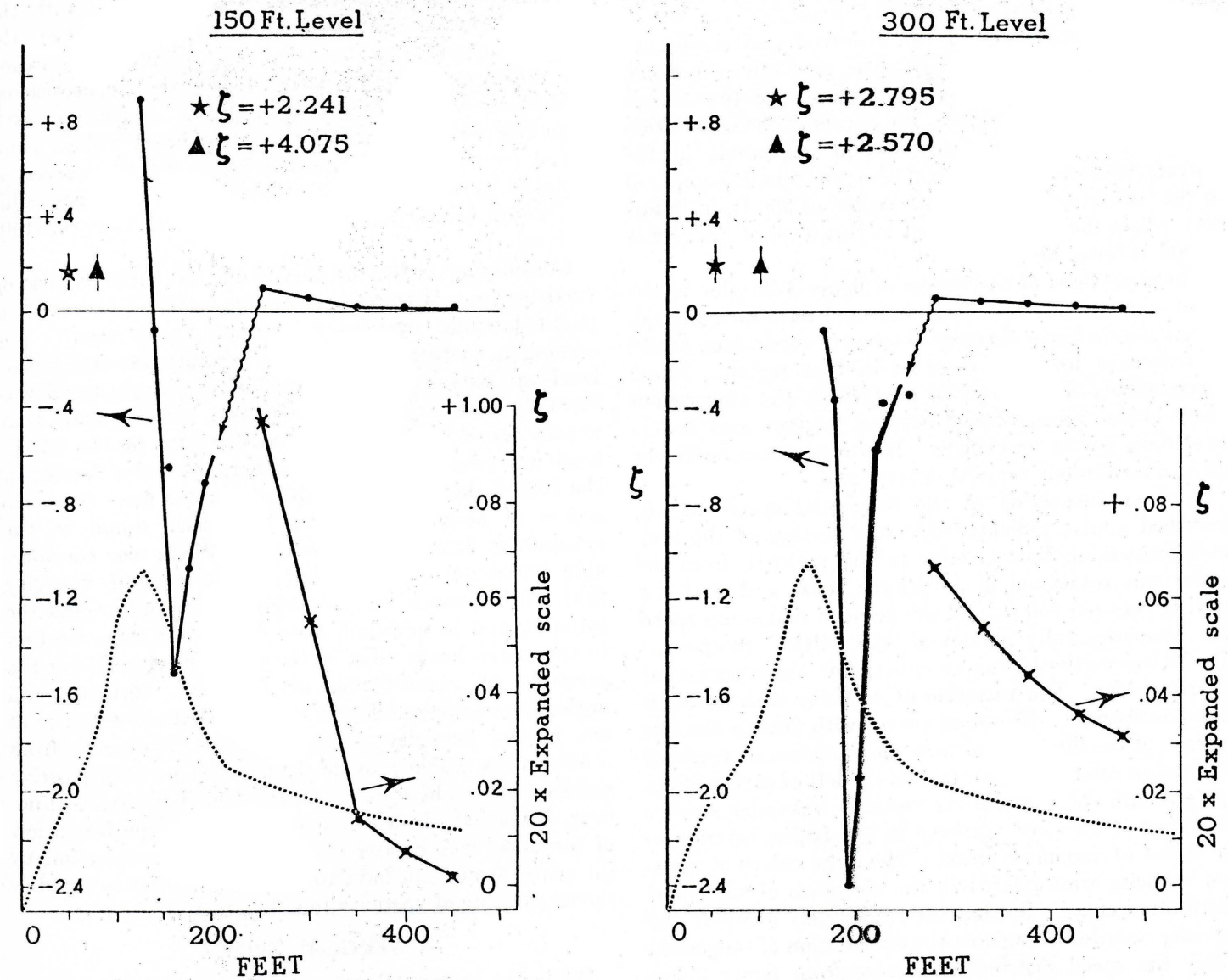


FIGURE 4.—Variation of vorticity with radius at the 150- and 300-ft. levels using tangential speeds from figure 3. A 20-times expanded scale is provided for the portion exterior to about 225 ft. in radius.

(dotted lines) on these graphs shows considerable deviation, indicating that the observed speed distributions were not irrotational. However, curves with  $VR^{0.8} = \text{Constant}$  are fitted to the shallowly sloped outer portions; the fit is very good, as shown by the open triangles. For interest these curves were continued inward nearly to the radius of observed maximum speed. No attempt was made to fit the steep, inflected inner curves with a simple mathematical curve. However, the slope was approximately averaged by the curve  $VR^{1.6} = \text{Constant}$  (dashed curve with circled dots).

The observed curves show that the air flow in the vortex exterior to the break in the curves (about 250-ft. radius) is rotational in the positive sense (cyclonic) and in the negative sense (anticyclonic) interior to the break point. It is presumed that surface and internal frictional effects used the slow rate of increase in speed inward between radii of 550 and 250 ft. and prevented the conservation

of angular momentum. Inward from the radius of maximum speed the deviation of the curves to speeds less than that required for solid rotation may reflect the effects of friction at the ground. However, the deviation is not great.

A rather accurate distribution of observed (derived) tangential speeds at 1000 ft. above the ground and out to a radius of 1360 ft. was provided by the tracking of cloud tags near that elevation at small intervals of radius. This distribution is shown in figure 3c as the solid curves with dots. The slope of this speed distribution curve is considerably more shallow than the slopes of the curves for the lower levels. Surprisingly enough, the portion of this curve exterior to the radius of maximum speed follows quite closely the theoretical  $VR = \text{Constant}$  curve (dotted line) as shown on the graph. The observed curve drops a little below the theoretical curve between radii of 290 and 575 ft., comes slightly above the theoretical curve



between radii of 575 and 1100 ft., and then again drops slightly below it beyond 1100 ft.

The near-conformity of the observed and theoretical curves at the 1000-ft. level indicates that the irrotational vortex apparently can exist in nature and that where conditions are removed from the effects of surface friction conservation of angular momentum is possible in the convergent vortex. The lag of observed speed (compared to the theoretical speed) in the region of 350 ft. in radius may reflect the retarding effect at this level of the slower speeds at lower levels.

Those portions of the curves of figure 3 interior to the point of maximum speed are inflected and, as analyzed, do not show a linear decrease of speed inward which would be necessary for solid rotation in that region. These curves reflect the manner of analysis in the core region where direct interpolation between higher- and lower-level data points was made. However, these nonlinear speed distributions may have been real.

Since an inspection of the tangential speed curves, described above, indicated that the portion of the low-level tornado air flow exterior to about 250 ft. from the center was rotational in a cyclonic sense and that the portion between 250 ft. and the point of maximum speed was anticyclonically rotational, the vertical component of relative vorticity was computed for these curves at several points. The variation of vorticity with radius is shown in figure 4. The solid curves with dots in the two sections of the illustration show the variation of vorticity with radius relative to the scale on the left of each section. The absolute value of positive vorticity was much smaller than that of negative vorticity in the region exterior to the radius of maximum speed. The large values of negative vorticity were related to the steepness of the speed distribution curve. So that the reader may compare the vorticity distribution against the distribution of tangential speed, the speed distribution curves from figure 3 are shown as dotted curves in figure 4. To show the radial variation of positive vorticity to better advantage, the vorticity values were plotted at the right-hand side of the graphs on a scale 20 times larger than the left-hand scale. The steeply rising curves (through crossed dots) to the right in each panel of figure 4 are fitted to the expanded scale. The vorticity distribution curves are discontinuous at the same locations that the speed distribution curves are discontinuous.

Since the observed and theoretical tangential speed curves coincided so closely at the 1000-ft. level no computations of vorticity distribution with radius were made for that level. However, two point determinations were made and were plotted on the curve of figure 3c. One at the 300-ft. radius was  $-1827 \times 10^{-4} \text{sec.}^{-1}$  in the region where the observed curve was steeper than the theoretical curve. Another at the 600-ft. radius was  $+303 \times 10^{-4} \text{sec.}^{-1}$  in the region where the observed curve was less steep than the theoretical (nonrotational) curve. Those portions of the flow inside the radius of maximum speed

indicate high positive vorticities as computed with the observed speed distribution of figure 3. Since the average steepness of the speed distribution curves inside the radius of maximum speed steepened with decreasing altitude the values of vorticity in that region also increased generally with decreasing altitude. Point values computed for the three levels are shown on the curves of figure 3, and are indicated on figure 4 at the proper radii. Maximum values exceeded  $4000 \times 10^{-3} \text{sec.}^{-1}$  for the 150-ft. level.

Considering orders of magnitude of these values of vorticity, one is reminded that an average figure for a middle-latitude cyclone is around  $2 \times 10^{-4} \text{sec.}^{-1}$ . Accordingly, the greatest positive vorticity for the 150-ft. level and exterior to the radius of maximum speed was virtually four orders of magnitude greater than that usually found in the cyclone and the value for the 300-ft. level was nearly as high. Further, the value found for the 1000-ft. level at the 600-ft. radius was more than two orders of magnitude greater than that found in the synoptic cyclone. This means that there was considerable horizontal concentration of the vertical vorticity field, that is, much vertical stretching in and around the tornado, and in addition, more horizontal concentration in the lower levels than in the upper levels. Using the principle of conservation of potential vorticity and neglecting compressibility it is found that convergence of air, having vorticity of the order of  $10^{-4} \text{sec.}^{-1}$ , from 5 miles away would provide the greatest value of positive vorticity found here at about the 250-ft. radius. However, if vorticity in a region favorable for the formation of tornadoes was greater than  $10^{-4} \text{sec.}^{-1}$  the advection to the center would not have to come from so far to provide the large value of vorticity found in this tornado.

### 3. VERTICAL SPEEDS

While the tangential wind speeds were being obtained by means of the cloud tags and the temporarily suspended solid debris particles (as in fig. 1), vertical components of motion were observed and measured in the cloud tags and it was realized that vertical motion of the air was required to suspend the solid objects. When cloud tags were tracked, the vertical speed of the tag was taken as the upward air current speed at the radius where it was found. When pieces of debris were tracked, some allowances were necessary regarding their terminal falling speed in still air. Fortunately, during the period that was investigated, the tornado had picked up, possibly from a lumber yard, a large number of thin sheets of material, all of which were about  $4 \times 8$  ft. in size. These objects were used for most of the low-level speed measurements. The movie showed that they were tumbling, which would give them a rather uniform falling rate. Hence, the falling rates of about a dozen of these pieces were measured when they appeared to be far enough from the tornado's influence to reach a nearly true terminal falling speed relative to a stationary atmosphere.



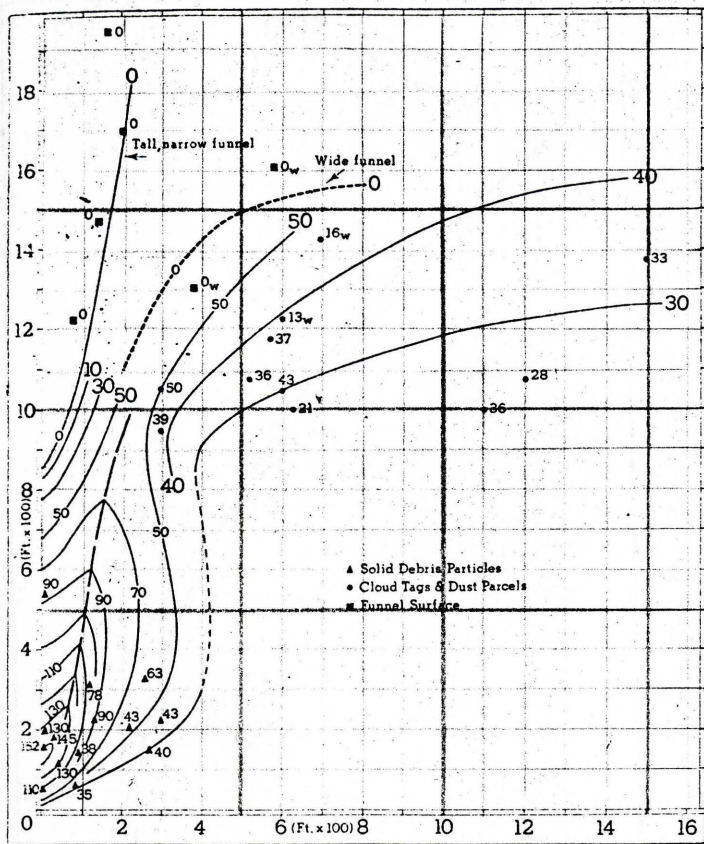


FIGURE 5.—Distribution of derived upward speed from the center of the tornado to about 1500 ft. in radius and from the ground to about 1700 ft. in elevation.

These speeds averaged 43 m.p.h., with only a little scatter. Accordingly, when any of these 4×8 ft. pieces were tracked for vertical speed, a correction of 43 m.p.h. was added algebraically to whatever vertical speed the particles had relative to the ground. The radius of the path was already available for each particle from the tangential component measurements. Since there are fewer data points for vertical speed than tangential speed, there is less confidence in the distribution of the vertical speed isotachs than for the horizontal speed isotachs in some portions of the tornado.

Figures 5 and 6 show the distribution of the upward speed data points around the tornado and the isotachs fitted to them. The center of the tornado is along the vertical scale at zero radius. Figure 5 shows the overall picture and figure 6 the lower 800 ft. in greater detail. The fit of the isotachs in figure 5 shows a relatively small low-level core of high-speed upward air flow at about the 135-ft. elevation. The maximum derived upward speed was 152 m.p.h. Above the high-speed jet at an estimated elevation of 850 ft., the upward speed became zero and from this point the zero isotach sloped upward with increasing radius in a manner, at any one time, apparently depending upon the shape and size of the funnel. Late in the lifetime of the tornado the zero-speed envelope was in a narrowly tapered shape somewhat as outlined by the

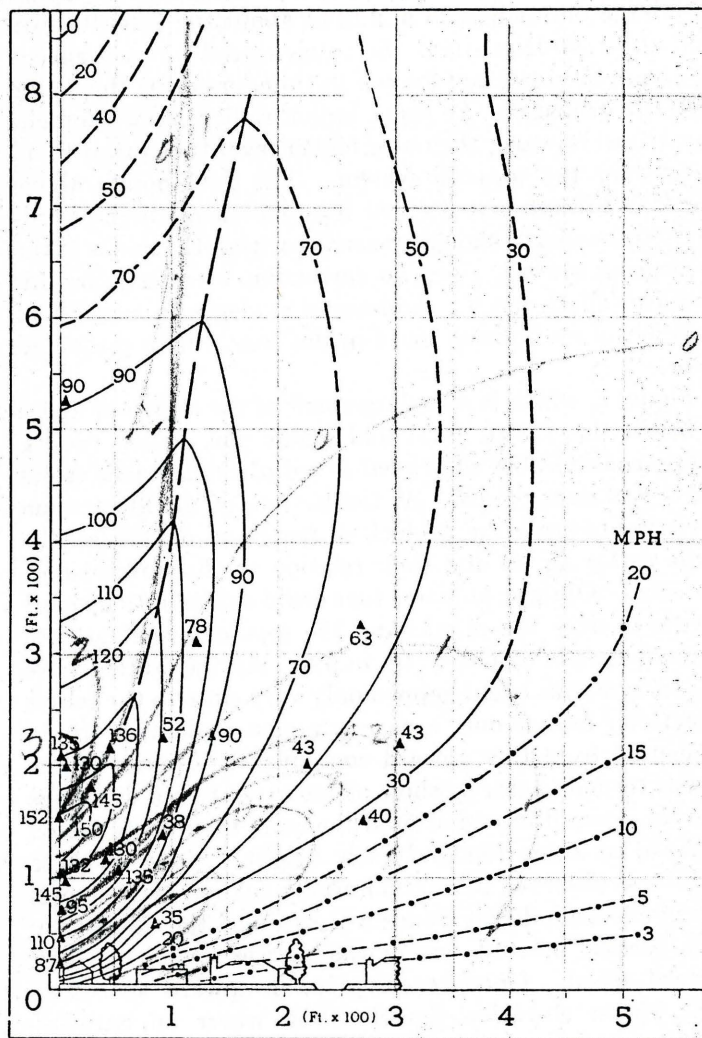


FIGURE 6.—Detailed version of distribution of upward speeds. Only the lower 900 ft. and the inner 500 ft. are shown.

zero isotach in the upper left of the diagram and labeled as "tall, narrow funnel." The condensation funnel at the later stage actually extended to the ground but it was impossible to determine the level at which zero vertical speed began in the core. At an intermediate time stage the zero-speed envelope lay approximately along the dashed curve in a form to agree with the zero upward speed data points marked with a subscript "w" and also agreeing with the shape of the funnel at that time. The zero speeds were found by tracking cloud fragments on the funnel surface. The "w" indicates that these data points were taken when the top of the funnel was wide compared to those taken at a later stage. The two upward-speed data points subscripted with "w", and located in the region of about 1300 ft. in elevation and 700 ft. in radius, have values much lower than surrounding data points. They were derived by tracking cloud parcels a relatively short distance from the condensation envelope at a time when the envelope was relatively wide.

In the region above the 900-ft. level and outside the 400-ft. radius the isotachs turn cutward and become



nearly horizontal. The greatest measured upward speed at a large radius was 33 m.p.h. at about the 1400-ft. level and the 1500-ft. radius. Since measured upward speeds of about 55 m.p.h. are known in thunderstorms this value is quite realistic. At some larger radius these isotachs must turn upward, then at a higher level turn inward and meet over the tornado system. The data points above the 900-ft. level were derived from cloud tags and accordingly these speeds should be correct within the limits of the measuring system, since no correction was necessary for particle falling speed. Additional evidence in support of a region of no upward speed in the core will be presented later.

Figure 6, which is an enlargement of the region of figure 5 below the 900-ft. level and inside the 500-ft. radius, shows considerable additional detail of the isotachs (solid lines) and data points. At the bottom of the illustration is shown to scale the  $\frac{1}{2}$  block of trees and dwellings (the same as for fig. 2) and their relation to the upward-flow isotachs. Observe how tree tops could extend into upward speeds of over 100 m.p.h. and the tops of dwellings into upward speeds of nearly 90 m.p.h. As the isotachs are shown here, this could happen only very close to the center of activity and so only a narrow region of damage would be caused from this upward component. Movies of the Dallas tornado actually show pieces of shattered dwellings moving upward in and around the core, then being tossed outward at some relatively low height. None of these pieces was observed to ascend initially outside of the dense, but small-sized, debris cloud; it is assumed then that they were carried upward within the narrow region of high upward speed. Upon reaching lower upward speeds at some higher elevation (an elevation where an outward component must exist), the pieces were ejected and then dropped since upward speed was insufficient to support them.

The data points near the center of the tornado and below 300 ft. in height show how the high speed upward current split into a cone-like form around the core (an arrangement that was mentioned earlier) such that above about 150 ft. in height the upward speed in the core was slower than the air immediately outside it. It was almost as if the air flow split around a pointed cone somewhat as around a sharp airplane nose. In the lower portion of figure 6 are some theoretical isotachs of vertical speed indicated by the dot-dash lines. They were included to show how nicely they fit with the observed isotachs. The procedure for generating them will be described later.

As will be seen in figure 6, some of the data points do not fit the analysis; examples are the ones at the 225-ft. level, 90-ft. radius (52 m.p.h.) and the 135-ft. level, 90-ft. radius (38 m.p.h.). The policy of showing all reasonable data points obtained (as was used for fig. 2) is retained here. The only exceptions were some points located below the 30-m.p.h. observed isotach that were much too high for both the observed and theoretical speeds.

In order to test the observed vertical speed distribution

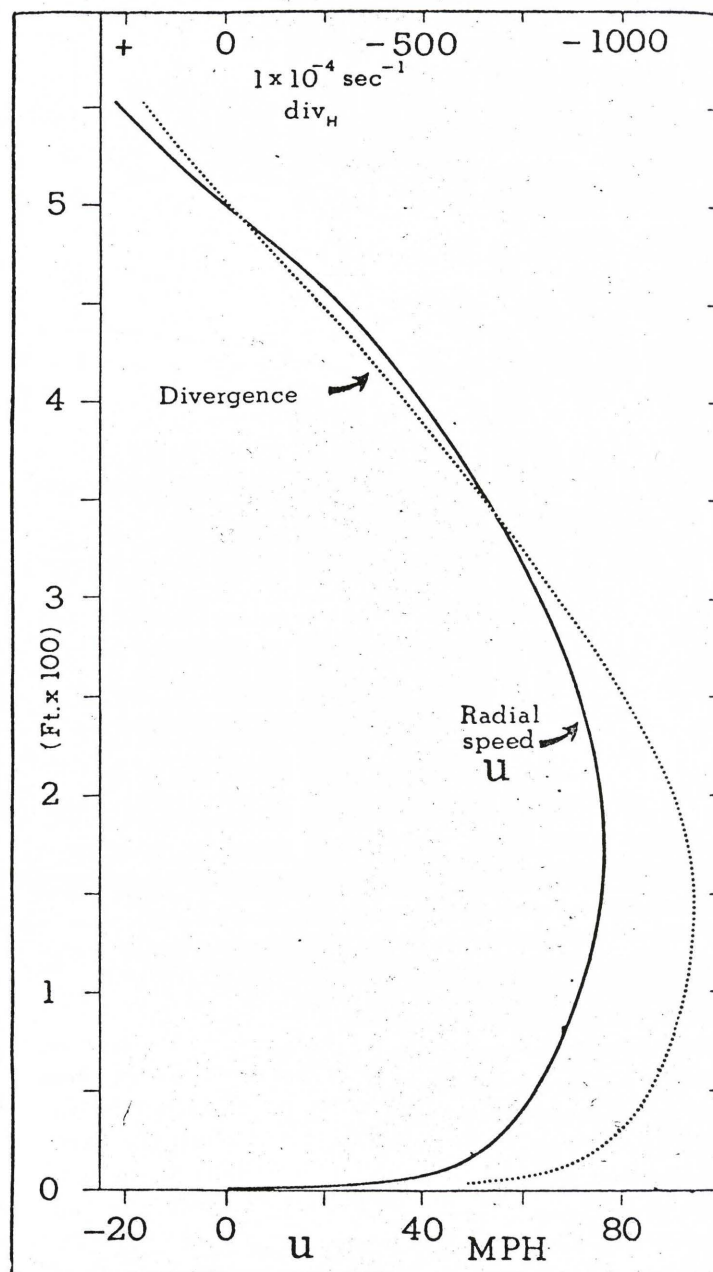


FIGURE 7.—Distribution of assumed radial speed,  $U$ , with elevation at the 500-ft. radius (solid line, using the scale at the bottom) and the distribution of horizontal divergence with height at the 500-ft. radius (dotted line using the scale at the top).

of figure 6 for consistency in the region exterior to the location of maximum upward speed and below 600 ft. in elevation, a theoretical vertical speed distribution was constructed. It was based on the principle of continuity, the assumption of incompressibility, and use of a convergent radial speed ( $U$ ) distribution of the form  $U \propto 1/R^n$ , where  $0 < n < 1$ ; inward flow is designated as positive in the following analysis. The assumed distribution of  $U$  with height at the 500-ft. radius was adapted from a graph of low-level wind-speed distribution with height, published by the Weather Bureau [6]. It was modified



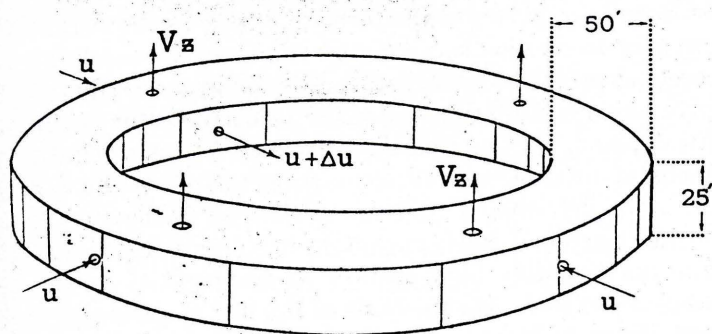


FIGURE 8.—Volume element used in computing theoretical upward speed distribution from the assumed radial speed distribution.

so that  $U$  reached a maximum at the 175-ft. level, decreased to zero at the 500-ft. level, and then reversed to outward flow above 500 ft. This distribution with height is shown by the solid curve in figure 7. The horizontal radial-component speed at 6.25 ft. above the ground and at the 500-ft. radius was taken as 40 m.p.h. and directed toward the center. The values of  $n$  used were 0.4 from the ground to 100 ft. in elevation, 0.5 from 100 to 200 ft. in elevation, and 0.6 for elevations above 200 ft., so as to be consistent at least qualitatively with decrease of frictional drag at increasing distances above the ground. Vertical speeds were computed from the time rate of excess volume accumulating in rings of unit volume around the tornado which were 50 ft. wide and 25 ft. deep, one of which is shown in figure 8. Above 212 ft. in elevation, the rings were 50 ft. deep. The vertical speed coming out of each ring was accumulated from the ground upward such that a distribution of vertical speed was obtained from the 500-ft. radius inward and from the ground to a little over 600 ft. in elevation.

The resulting distribution of computed upward speeds with height and radius is shown by the solid curves of figure 9. Not all the computed data points are shown but the isotachs were drawn with all of them in consideration. For comparison with the isotachs of theoretical upward speeds, the observed speeds from figure 5 are reproduced as dashed lines in figure 9. Considerable agreement is shown by the near fit on the 30-, 50-, and 70-m.p.h. isotach lines. But the 90-m.p.h. observed isotach is considerably nearer the center of the tornado than is the theoretical line. Nevertheless, where agreement in speed is poor the trend of the theoretical and observed lines is nearly the same. Increasing the radial speed  $U$  inward from about the 250-ft. radius only, and keeping the outer portions as described above, brought the 90-m.p.h. theoretical isotach into near coincidence with the 90-m.p.h. observed isotach and at the same time kept the 30-m.p.h. isotachs in close proximity. However, the 70- and 50-m.p.h. theoretical isotachs moved inward away from their positions of near coincidence in figure 9, and the computed isotachs lost their smoothly curved characteristics. Undoubtedly distributions of  $U$  with

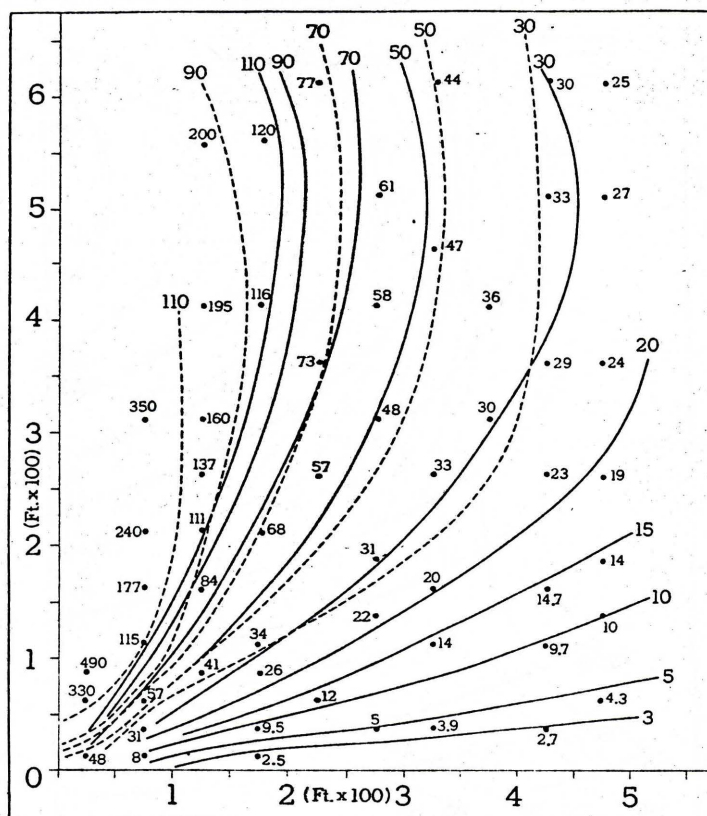


FIGURE 9.—Distribution of theoretical upward speed (solid lines) computed from the assumed radial speed distribution of figure 7 (solid curve). Dotted lines are isotachs of observed upward speed.

radius could be devised that would give even better approximations than those shown here, but the effort to find them is time consuming. Here at least, it has been shown that a good approximation to a portion of the observed distribution is possible. Perhaps if the volume of air specified by the method did truly ascend in the middle of the tornado the observed upward speed distribution near the center would more nearly coincide with the theoretical distribution. Very likely the separation of the vertical high speed jet into a shell around the less speedy tornado core at high levels accounts for the observed increase being less rapid than the theoretical increase of upward speed inward from about the 200-ft. radius.

For the purpose of comparison of convergence in other observed tornadoes and thunderstorms, the convergence in the specified horizontal wind system of the Dallas tornado was computed. The computation was made at the 500-ft. radius and in steps from 6.25 ft. to 550 ft. above the ground. The same radial speed distribution with height was applied that was used in constructing the theoretical vertical speed distribution (see fig. 7). The convergence values range from  $700 \times 10^{-4} \text{ sec.}^{-1}$  at 6.25 ft. above the ground to a maximum of  $1175 \times 10^{-4} \text{ sec.}^{-1}$  at about 150 feet above the ground. The results are displayed on figure 7 as the dotted curve with the scale



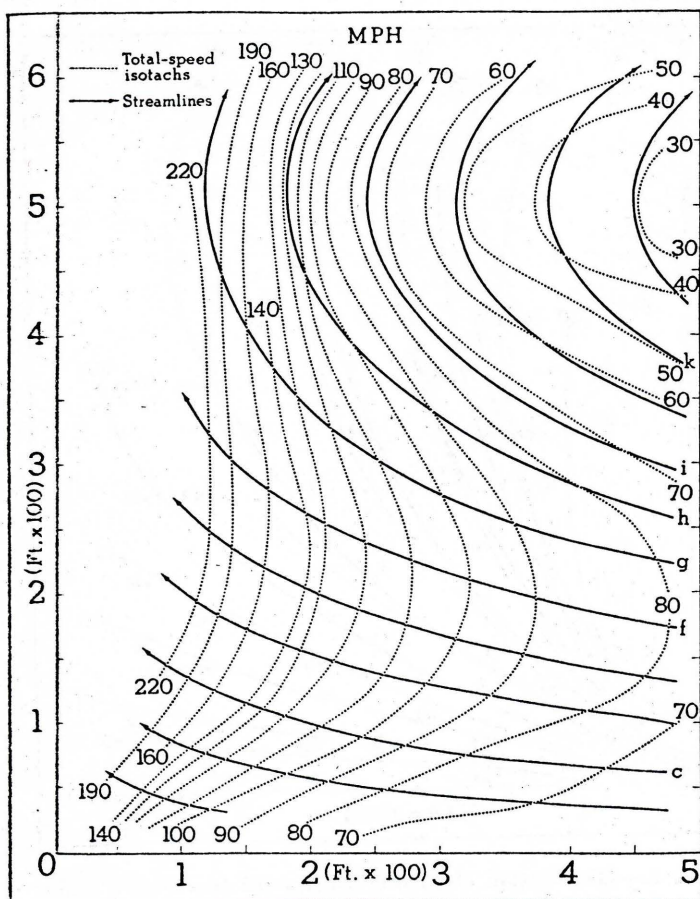


FIGURE 10.—Computed trajectory and isotach pattern in the vertical plane through the lower portion of the tornado.

at the top of the graph applying. Convergence went to zero at the 500-ft. elevation as required by the distribution of  $U$  in figure 7. The maximum value quoted above is approximately four times greater than the convergence found by Fujita [4] in the Fargo, N. Dak., tornado of June 20, 1957, at a radius of about 3000 ft. and an elevation of 3000 ft. Convergence in the Dallas tornado was also computed from derived radial wind components obtained from movement of industrial smoke plumes near the tornado (Hoecker [7]) for a radius of 0.75 mile and elevation of about 600 ft. These values were around  $350 \times 10^{-5} \text{ sec.}^{-1}$ , about 1/35 of the maximum value computed above from synthesized values of radial speed (see fig. 7) at the 500-ft. radius. Additional comparison comes from data obtained in the Thunderstorm Project [2], where it was found that precipitating Florida thunderstorms provided convergence between  $250 \times 10^{-4} \text{ sec.}^{-1}$  and  $550 \times 10^{-4} \text{ sec.}^{-1}$ , the latter between 16,000 and 20,000 ft. in elevation. The larger figure for the thunderstorms was about two-thirds of that found for the Dallas tornado at the 150-ft. level and 500-ft. radius, using the synthesized inflow data.

Inasmuch as the theoretical distribution greatly resembled the observed distribution of upward speeds, at

least in certain regions of the tornado, it was assumed that the synthesized radial speed distribution and the resultant theoretical upward speed distribution could be combined to give a realistic distribution of the velocity vector in the vertical plane. From this distribution of vector winds, isotachs of total speed and some trajectories\* in the  $r$ - $z$  plane were determined and are displayed as figure 10. The inner portion was left vacant, as it was earlier, because of the unreasonably high upward speed required by the synthesized model. On the basis of the initial assumption stated above, it is presumed that the trajectory analysis of figure 10 closely resembles the actual trajectories that existed at times in the tornado flow.

As shown in figure 10, the trajectories have a definite upward component throughout the region represented; this is required for the convergent regime of the radial component of wind. And, as required by the distribution of  $U$  with height (shown as the solid line of fig. 7) the trajectories show a reversal to outward flow above the 500-ft. level. Note that the curvature of the trajectories at the 500-ft. level is greater at larger distances from the tornado. Trajectories entering the illustration from the right below 300 ft. in height cross over to regions of greater speed while those entering above 300 ft. cross over to regions of lower speed ending at the 500-ft. level. Above 500 ft. they enter regions of increasing speed. There is the suggestion of a closed circular movement of air in the shape of a ring vortex around the tornado, having a horizontal axis at the 500-ft. level and a little outside the 500-ft. radius. This suggestion is augmented by the shape and movement of the outer and upper edge of the more dense debris cloud where in both still pictures and movies an outward and downward curling motion takes place. This curling action is typified in the upper right-hand portion of the schematic debris cloud shown in figure 1.

Mass divergence in the steady-state system of figure 10 is required to be zero, but attempts to prove this encounter difficulties such as determining the distribution of density in the system. However, on an assumption of incompressibility, zero velocity divergence was imposed on the system by the manner of determining the upward speed distribution from the elemental volumes of figure 8.

#### 4. THE THREE-DIMENSIONAL FLOW

The vector flow distribution in three dimensions below the 600-ft. level and inward from the 500-ft. radius was determined using the vertical plane trajectories of figure 10 and horizontal streamlines. The horizontal streamlines at given levels were obtained by vector addition of the computed radial component regime, described earlier, and the observed tangential wind speed. Again the assumption was used that since the computed upward speed distribution closely resembled the observed upward speed distribution (at least outside the central core region) the synthesized radial speed distribution closely resembled the

\*Because of the implicit steady-state assumption, streamlines and trajectories coincide.



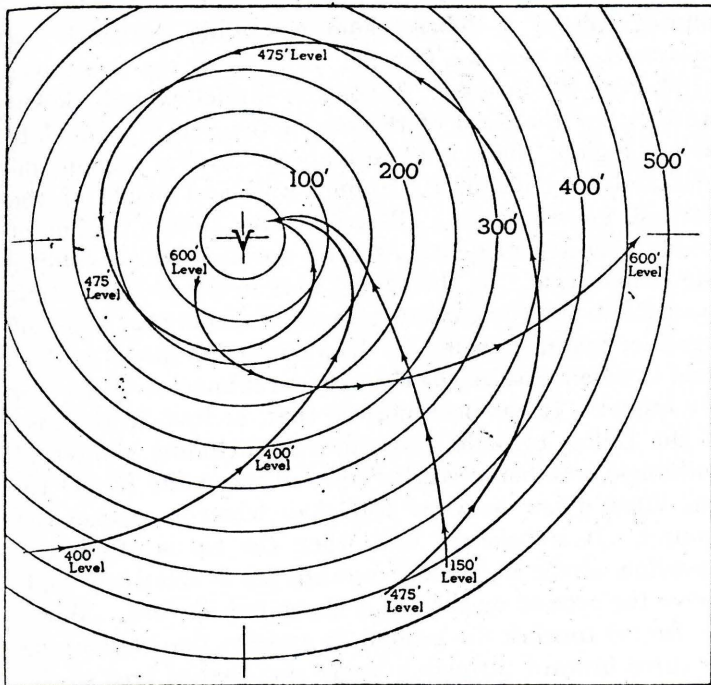


FIGURE 11.—Horizontal streamline patterns for several levels of the tornado in the lower 600 ft.

actual, but unmeasurable, radial wind speed distribution. Horizontal streamline patterns were computed for 50-ft. vertical intervals from 50 ft. in elevation to 600 ft. in elevation with an additional level at 475 ft.; some of the significantly different patterns are shown in figure 11. In order to emphasize the differences in streamline curvature with elevation the end points of the several streamlines have been made to coincide. Note the predominantly radial component for the 150-ft. level and the increased tangential component at the higher levels. The horizontal streamlines for the 500-ft. level would, of course, be concentric circles. At the 600-ft. level the streamlines are divergent as indicated in the figure.

The horizontal projection of some of the three-dimensional trajectories are shown in figure 12. Along each trajectory are shown the starting elevation and the points at which the trajectory passed each 50-ft. level. (The crossed dots are not data points.) The key letters at the start of each trajectory refer to identically keyed trajectories in the  $r$ - $z$  plane of figure 10. These trajectories were constructed by following the horizontal streamline pattern in each 50-ft. vertical interval bracketing a standard level (i.e., 75 to 125 ft. for the 100-ft. level, etc.). Segments for each height interval were connected resulting in the trajectories of figure 12. The radius of each segment was controlled by the corresponding trajectory in figure 10.

One of the interesting features of these trajectories is the generally small curvature in the horizontal plane. Only trajectories "c" and "f" curve sharply and then only inside the 150-ft. radius. The others seem merely to cut across an edge of the tornado.\* Trajectory "i"

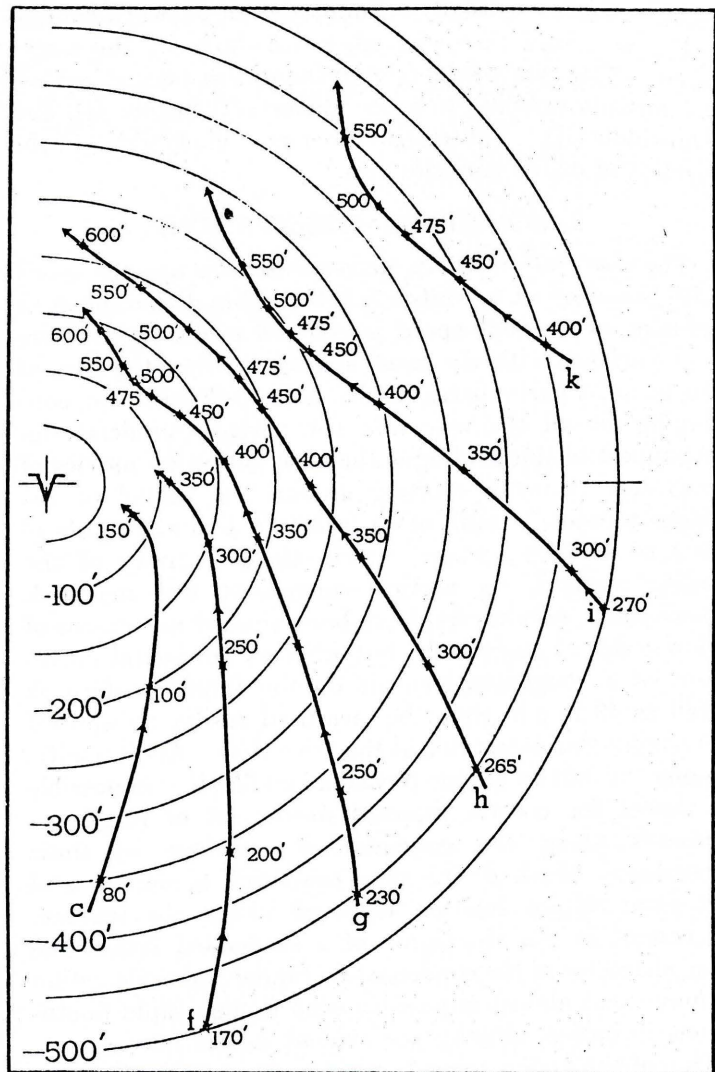


FIGURE 12.—Horizontal projections of the three-dimensional trajectories of some air parcels which also follow the trajectories of the vertical projection in figure 10. Key letters identify identical trajectories in figures 10 and 12.

through part of its track is convex to the tornado and trajectory "k" is entirely convex. These trajectories show that in the region below the 500-ft. level and at the 500-ft. radius, the higher the entry elevation for the air parcel the less closely it approached the center of the tornado. Unfortunately, the radial inflow assumption did not generate the observed vertical components in the center of the tornado and so the trajectories in that region were not computed.

It is thought that the three-dimensional trajectories are quite representative since there was some similarity between the trajectories of figure 12 and the paths of the particles flying around the tornado, as seen in one of the Dallas tornado movies. In the movie the particles are, in many cases, thrown out ahead of the tornado in the direction of its motion after having been lifted into the circulation. As the particles were brought inward and upward, they entered a region of decreasing inward com-

\* Illustrating the domination of tangential speeds over radial speeds except in the lowest 100 ft.



parent wind, eventually encountered an outward component, and were then ejected, particularly at the larger radii. This type of debris movement has been described by tornado eyewitnesses (see Bigler and Segner [1], and Dinwiddie [3]). Centrifugal force most likely aided in the ejection of debris particles also.

### 5. NONTYPICAL OBSERVATIONS

The observation of the decrease of core upward speed with elevation at a relatively low level and the apparent splitting of the high-speed jet around a less speedy core is at variance with the usual conception that the core of the tornado participates in the sink mechanism for converging air all the way into the parent thunderstorm. In support of this finding is the observation by movies of roughness elements rotating around the funnel of the Dallas tornado at radii of 75 to 200 ft. and at heights of 1500 to 1900 ft., where, within the sensitivity of the scaling method, no vertical movement was detected. There could, admittedly, have been upward movement of a low order of magnitude, but whereas horizontal movement of a roughness element on the funnel surface as small as 40 m.p.h. could be measured easily, no upward movement was detectable at the same time. Additionally, among the movies of four tornadoes on file, it is impossible to detect for certain, upward movement of roughness elements along the condensation envelope of these tornadoes. Much of the time the trunk is smooth and not even ripples can be detected along the surface. Of course, in the tip region of a suspended funnel the hazy character of the condensation funnel makes detection of movement almost impossible even though rapid fluctuations in optical density are evident in the movies.

One of the Dallas tornado movies shows upward movement of optical density discontinuities in the hazy, lower portion of the suspended tip region when it was several hundred feet above the ground and quite narrow. The upward jet was feeding into the condensation trunk tip region at this time and possibly was effective in hindering condensation there. Upward speed did not appear to increase with elevation along the flow path. An observation at very close range by Dinwiddie [3] of a waterspout-turned-tornado agrees qualitatively with the observed upward speed distribution indicated by figure 6 in the region below the 300-ft. level and inward from the 100-ft. radius. Dinwiddie describes objects being carried aloft to a certain level, being momentarily suspended, then ejected outward and downward. He concluded that there was a high-speed upward jet close to the ground whose upward speed eventually decreased with height.

Many still photographs of tornadoes and their attendant debris clouds indicate that the major sink region is exterior to the condensation funnel. For example, when the condensation trunk tip is at or near the ground the width of the rotating debris cloud is greater than when the trunk is suspended aloft. The writer has never seen a

photograph of a debris cloud extending outward and upward from *within* a tornado trunk while the trunk was at or near the ground. When the funnel extends downward below the level of the top of the dense particulate debris region, there is almost always a clear region immediately outside of the funnel wall and inside of the darkest debris region. This indicates that a region of greater density of debris extends upward while avoiding the funnel itself. If the funnel were involved in the sink mechanism for the cases observed, it seems that some of the finer material would be drawn into the funnel and so tend to de-emphasize the clear region immediately around the funnel. It has been noticed that, at least in the case of the Dallas tornado, more debris (including chunks of buildings) was being carried upward when the funnel tip was lifted a few hundred feet than when it was on the ground. It is believed that when the tip is lifted, the elevation of the high-speed upward jet is relatively high above the ground or at least is elongated upward. When the funnel touches the ground, it appears that converging air turns upward through a larger ring-shaped area so the maximum upward speed for a given sink strength is reduced and no central high speed core exists. However, upward speed is still sufficient to lift some lighter debris. Observational evidence in support of this idea is contained in a sequence of photographs of another tornado on file which showed the ground-based debris cloud increasing in diameter as the suspended funnel widened and lowered toward the ground. No debris was seen to rise in the region beneath the cut-off tip of the condensation funnel but all of it ascended exterior to the tapered cylindrical funnel which widened upward. In the pictures and movies of the Dallas tornado no large clouds of dust or spray, or chunks of structures were observed ascending along the trunk when the trunk was touching the ground. Had any large chunks been carried upward inside the funnel, surely a few would have been thrown outward through the funnel wall by centrifugal force much as they were observed to do when the funnel tip was retracted.

As a means of explaining a decrease of upward speed with height above the low-level high-speed core, the following idea is suggested: If the bent-down isobaric surfaces in this tornado were spaced, in the vertical, farther apart at the center than at larger radii, then there would be less upward accelerating force in the center. For example, if at some location spacing allowed an upward pressure gradient force that just balanced the pull of gravity, there would be no net upward force (excepting frictional force) on the air at that location and so a decelerating tendency would take place.

Some question undoubtedly arises as to the mechanism that removes the volume of air that continuously flows toward the tornado center in the lower levels. It is suggested that the flow in the tornado must take on an outward component above the level of maximum upward speed. This would allow the narrow, low-level upward jet to spread out over a larger area at higher elevations so



that a lower-speed, larger-area updraft around the tornado could easily remove upward the low-level convergent volume. The flattening out of the observed updraft isotachs around the tornado at higher elevations and larger radii shows some evidence for this suggested mechanism.

A rough volumetric test was performed to compare the flow rate through the 1200-ft. level out to 1600 ft. of radius with that through a surface at the level of the maximum-speed jet (150 ft.) out to 300 ft. of radius using upward speeds from figures 5 and 6. A uniform upward speed of 30 m.p.h. was used for the upper surface, 120 m.p.h. for the inner 100 ft. of radius, and 70 m.p.h. for the outer 200 ft. of radius for the lower level. Incompressibility was assumed. The flow rate through the upper surface computed to more than one order of magnitude greater than that through the lower surface. The upward speed used for the upper surface is a minimum and therefore the sink at 1200 ft. as computed would take care of a source strength more than ten times as great as provided by the lower surface.

It is also possible that some of the low-level air recirculates as is suggested by the turning outward and downward of the outer rim of the low-level dense debris cloud. This would require less volume to be removed at higher levels.

The reversal of radial inflow to one of outflow at some elevation (for this case, estimated to be at 500 ft. above the ground) is also at variance with generally accepted ideas of tornado flow mechanics. However, general spreading of the lighter debris particles with height up to the tornado-associated cloud base is indicated in many tornado photographs and is demonstrated in movies. If general indrafts into the trunk existed around this region there should be a concentration of the lighter material around the upper portion of the tornado and a tapering inward with height of the lightly shaded (that portion offering low optical density) and higher-level debris cloud. Such has not been found in the Dallas tornado photographs. However, in some tornadoes optically dense debris has been photographed ascending along the tornado trunk in a cylindrical shape as contrasted to the tapered outward and upward shape that so characterized the dense debris cloud of the Dallas tornado. In those cases the trunk was usually lowered to near the ground and was quite wide, and it is thought that such instances represent a particularly energetic stage of the tornado. The effect seen may be in the nature of a transient surge of air inward at low level and upward along the trunk which carries heavier particulate debris to higher elevations. Evidently the air flow pattern of the tornado is complex and changes from one tornado to another and may change from time to time in any one tornado.

## 6. CONCLUDING REMARKS

For the first time a distribution of observed tangential and upward air speed in a tornado has been obtained.

This was made possible by the use of tornado movies of high quality and the utilization of the methods of photogrammetry and perspective. Further, a convergent radial speed distribution was synthesized that produced an upward speed distribution quantitatively close to the observed upward wind speed distribution in the lower 600 ft. of the tornado. The three components (i.e., synthesized radial distribution, generated upward distribution, and observed tangential distribution) were combined to determine the three-dimensional air parcel trajectories for the lower portion of the Dallas tornado. These trajectories resemble the paths of some of the solid debris particles which were thrown out ahead of the right-hand side of the tornado after being lifted in the core.

From the analysis of the radial distribution of the tangential speed, vorticity distribution was determined at three levels. Large values of negative vorticity were found at small radii (but exterior to the radius of maximum tangential speed) and at low levels, and the  $VR = \text{Constant}$  relationship did not hold. At the 1000-ft. level, however, the  $VR = \text{Constant}$  distribution was nearly attained. Immediately outside of the region of maximum speed and at 150 and 300 ft. in elevation, the speed change with radius approached a  $VR^{1.6} = \text{Constant}$  relationship, while at greater radii a  $VR^{0.8} = \text{Constant}$  relationship was evident.

Extremely high tangential speeds were not found and 170 m.p.h. was the maximum, although there may have been higher speeds where tracers were not tracked or were absent.

The upward speed distribution was found to have a jet of maximum speed at about 135 ft. above the ground at the core; it decreased above that to zero near the 1000-ft. elevation. At a radius of 300 ft. the maximum upward speed in the lower levels was at the 400-ft. elevation, however. An envelope of zero upward speed was found above the 1000-ft. level which appeared to coincide with the condensation envelope.

Evidence was found in the distribution and movement of small particulate debris around the tornado to indicate that the upward flow took on an outward component above the region of maximum upward speed.

Some nontypical observations showed that no upward air flow was detectable on the surface of the funnel at levels above about 1000 ft.; only tangential components were detected. A suggestion was made that the condensation funnel, with the exception of the lowest portion of the suspended tip section, does not participate in the upward sink mechanism. Evidence in support of this idea is contained in movies and still photographs showing more debris being carried upward beneath the suspended funnel than when the funnel was on the ground and in sequential photographs showing a widening of the debris cloud into a ring shape at the ground as the funnel lowered and widened. The diameter of the debris cloud at ground level equaled or exceeded the diameter of the lower end of the condensation funnel.



The implication is that had the region in and beneath the lowering and widening funnel been involved in the sink, the debris would have converged to a small region beneath the lowering funnel rather than being turned upward at some larger diameter. The visible funnel does not control the sink distribution but only exists in the region of little or no upward air movement. Certainly air ascends in the vortex core beneath the suspended funnel tip and ascends around the exterior of the funnel whether it is suspended aloft or is on the ground.

Hence the air speed in the unmeasurable tornado has finally been measured and the speed distribution compared with theoretical distributions. To what extent other tornadoes differ from the Dallas tornado is not known but the disposition of the condensation funnel and the attendant debris cloud in other tornadoes indicates that some differences in degree must exist between individual tornadoes.

It is hoped that other high-quality movies of yet unborn tornadoes will be forthcoming so that treatment similar to that provided in this paper can be made.

#### ACKNOWLEDGMENTS

The author wishes to express his appreciation to Mr. William A. Hass for his interest in this study and for help-

ful discussions and comments, and to the several movie photographers for contributing their excellent movies of this tornado from which the raw data for this study were taken.

#### REFERENCES

1. Stuart G. Bigler and Edmund P. Segner, Jr., "The Dallas Tornado of 2 April 1957, Raw Data Report," *Scientific Report No. 2* on Contract Cwb-9116, Department of Oceanography and Meteorology, The Agricultural and Mechanical College of Texas, College Station, Tex., August 1957. (See pp. 193-230.)
2. H. R. Byers and R. R. Braham, *The Thunderstorm*, U.S. Weather Bureau, Washington, D.C., June 1949, 282 pp. (pp. 32-33).
3. Frank B. Dinwiddie, "Waterspout-Tornado Structure and Behavior at Nags Head, N.C., August 12, 1952," *Monthly Weather Review*, vol. 87, No. 7, July 1959, pp. 239-250.
4. Tetsuya Fujita, "A Detailed Analysis of the Fargo Tornadoes of June 20, 1957," *Research Paper No. 42*, U.S. Weather Bureau, Washington, D.C. (in press). (See Chap. 4.)
5. R. G. Beebe, "The Life Cycle of the Dallas Tornado," pp. 3-51 of "The Tornadoes at Dallas, Tex., April 2, 1957," *Research Paper No. 41*, U.S. Weather Bureau, Washington, D.C., 180 pp. (in press).
6. U.S. Weather Bureau, *Meteorology and Atomic Energy*, U.S. Atomic Energy Commission, July 1955, 163 pp. (p. 22).
7. W. H. Hoecker, Jr., "The Dimensional and Rotational Characteristics of the Tornadoes and Their Cloud System," pp. 53-113 of "The Tornadoes at Dallas, Tex., April 2, 1957," *Research Paper No. 41*, U.S. Weather Bureau, Washington, D.C., 180 pp. (in press).